iScience, Volume *24*

Supplemental information

Role of NKG2a/c^{+}CD8^{+} T cells in pathogenic versus non-pathogenic SIV infections

Nicolas Huot, Philippe Rascle, Nicolas Tchitchek, Benedikt Wimmer, Caroline Passaes, Vanessa Contreras, Delphine Desjardins, Christiane Stahl-Hennig, Roger Le Grand, Asier Saez-Cirion, Beatrice Jacquelin, and Michaela Müller-Trutwin

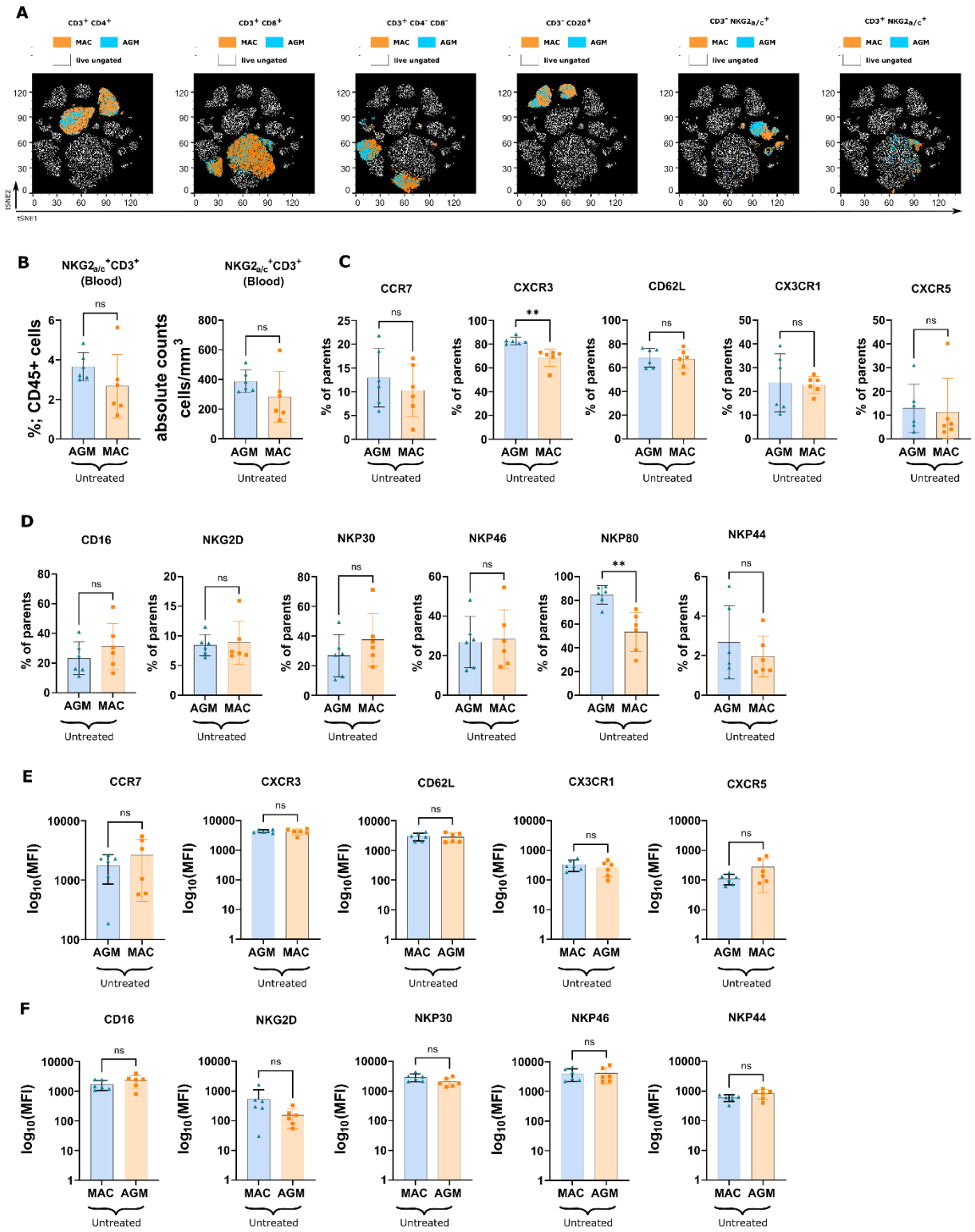

Supplemental Figure 1: Comparisons of NKG2$_{a/c}^{+}$CD8^{+} T cell blood phenotype between AGM and MAC. Related to Figure 1. **(A)** viSNE analysis on the concatenated flow cytometry data for 12 markers on peripheral blood mononuclear cells analyzed in 6 AGMs and 6 CMs. viSNE analysis was run on 120,000 live CD45^{+} single concatenated viable cells from monkeys and subjected to the *t*-distributed stochastic neighbor embedding (*t*-SNE) algorithm. Each dot plot represents the distribution of total cells (white dots). For each dot plot, the sub-population of cells of interest is highlighted in blue for AGM and orange for MAC. The population highlighted is defined at the top of each dot plot. **(B)** Graphs showing the comparisons of blood NKG2$_{a/c}^{+}$CD8^{+} T cells frequency (left panel) and absolute count (right panel) between healthy AGM (blue) and MAC (orange). Comparisons of the frequencies **(C) (D)** and MFI **(E) (F)** of homing and NK cell markers measured on blood NKG2$_{a/c}^{+}$CD8^{+} T cells between healthy AGM (blue) and MAC (orange). For all graphs, each dot represents an individual monkey. Bars represents the mean, and error bars indicate the standard deviation. Statistical significance of differences was assessed using non-parametric Mann-Whitney *U* tests, *$p < 0.05$, **$p < 0.005$, ***p<0.0005.

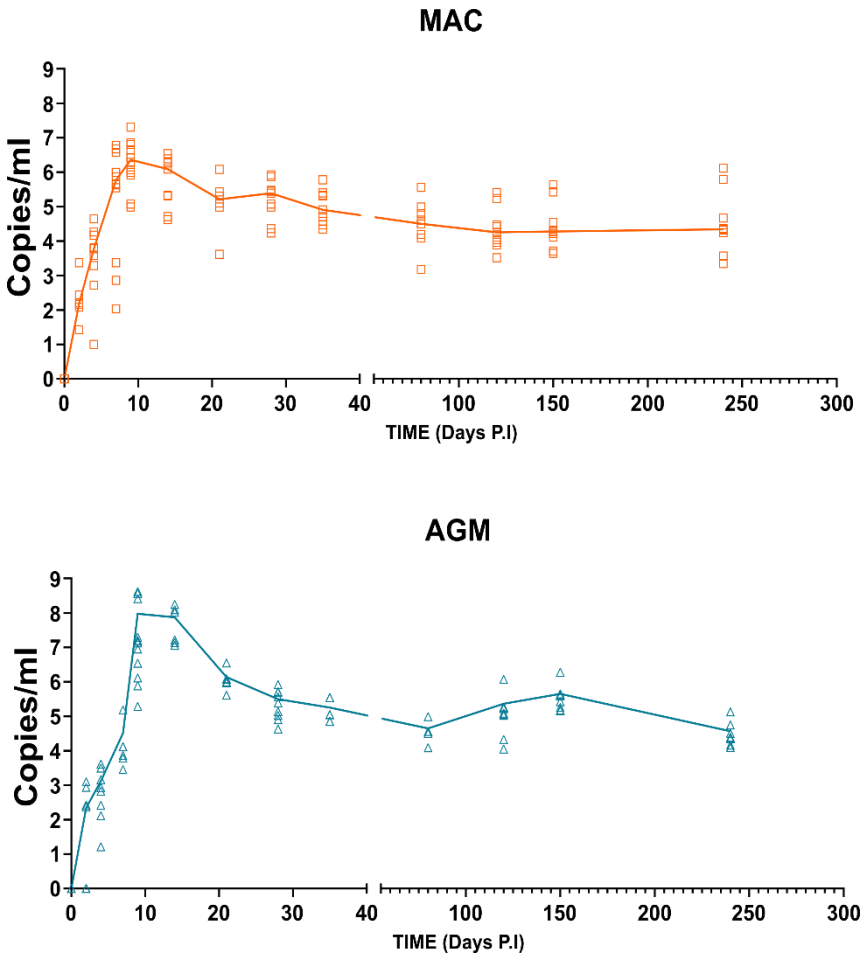

Supplemental Figure 2. Plasma viral RNA copy numbers in the longitudinally followed animals Related to Figure 2. The longitudinal studies included 12 cynomolgus macaques (CM) infected with SIVmac251 and 12 AGM infected with SIVagm.sab92018. The animals were followed until 240 days p.i. except for three per species that were sacrificed at day 9 p.i. for tissue collections in the acute phase of infection. The same animals have already been served for other studies.(Huot et al., 2017, 2020)

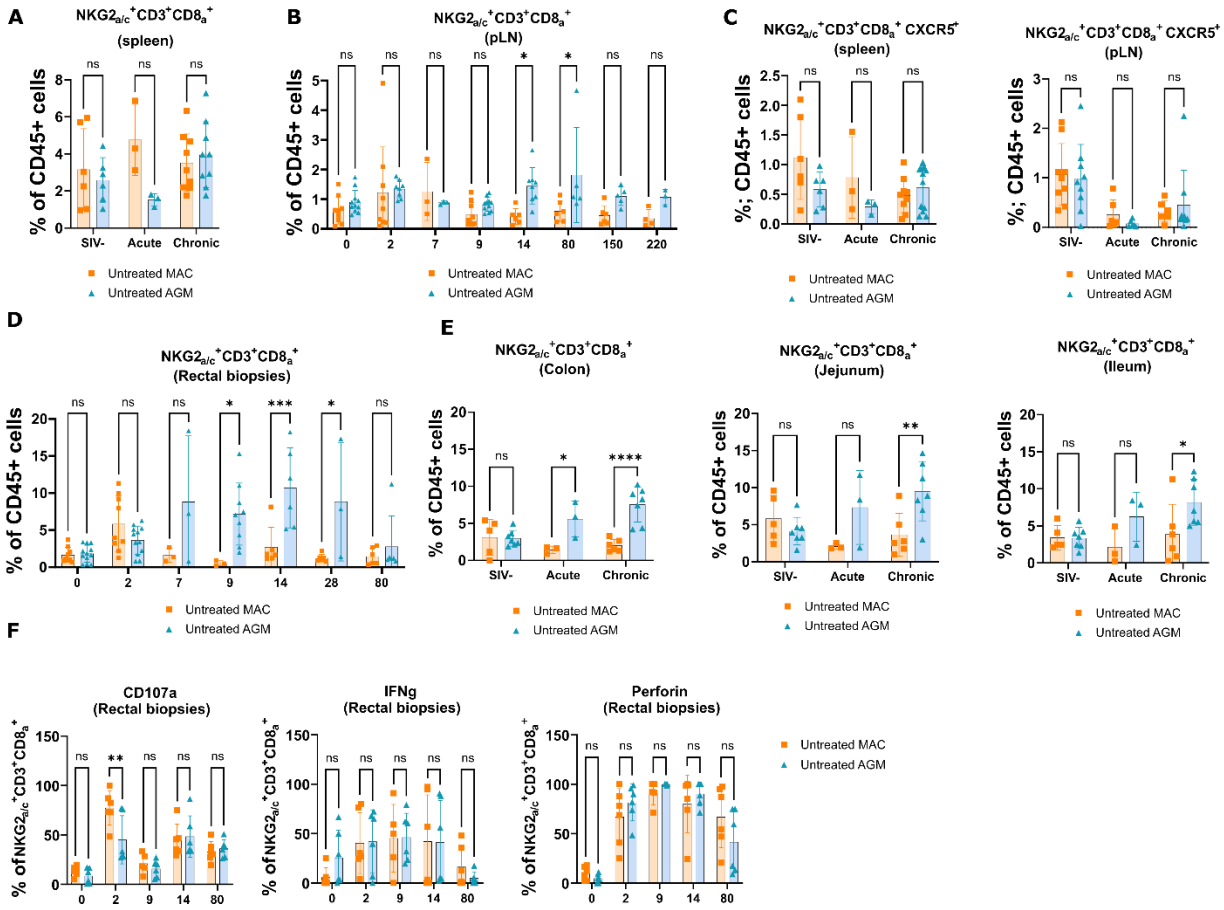

Supplemental Figure 3. Comparisons of tissue NKG2$_{a/c}^{+}$CD8^{+} T cell frequencies and phenotypes between AGM and MAC Related to Figure 4. Graphs showing the comparisons in (**A**) spleen and (**B**) pLN NKG2$_{a/c}^{+}$CD8^{+} T cell frequencies between AGM (blue) and MAC (orange) before, during acute and chronic SIV infection. (**C**) Graphs showing the comparisons in spleen (left panel) and pLN (right panel) of NKG2$_{a/c}^{+}$CD8^{+} CXCR5^{+} T cell frequency between AGM (blue) and MAC (orange) before and during acute and chronic SIV infection. (**D**) Comparisons of rectal biopsy's NKG2$_{a/c}^{+}$CD8^{+} T cell frequency between AGM (blue) and MAC (orange) before and at the indicated time point during SIV infection. **(E)** Graphs showing the comparisons of NKG2$_{a/c}^{+}$CD8^{+} T cell frequency in colon (left panel), jejunum (middle panel) and ileum (right panel), between AGM (blue) and MAC (orange), before, during acute and chronic phase of SIV infection. **(F)** Comparisons of NKG2$_{a/c}^{+}$CD8^{+} T cell frequencies positive for CD107a, IFNg, and Perforin in rectal biopsies between AGM (blue) and MAC at the indicated time point before and during SIV infection. For all graphs, each dot represents an individual monkey. Bars represents the mean, and error bars indicate the standard deviation. Statistical significance of differences was assessed using one-way analysis of variance (ANOVA) and followed by a Tukey's multiple-comparison test. The latter is a post-hoc test based on the studentized range distribution. *$p < 0.05$, **$p < 0.005$, ***p<0.0005.

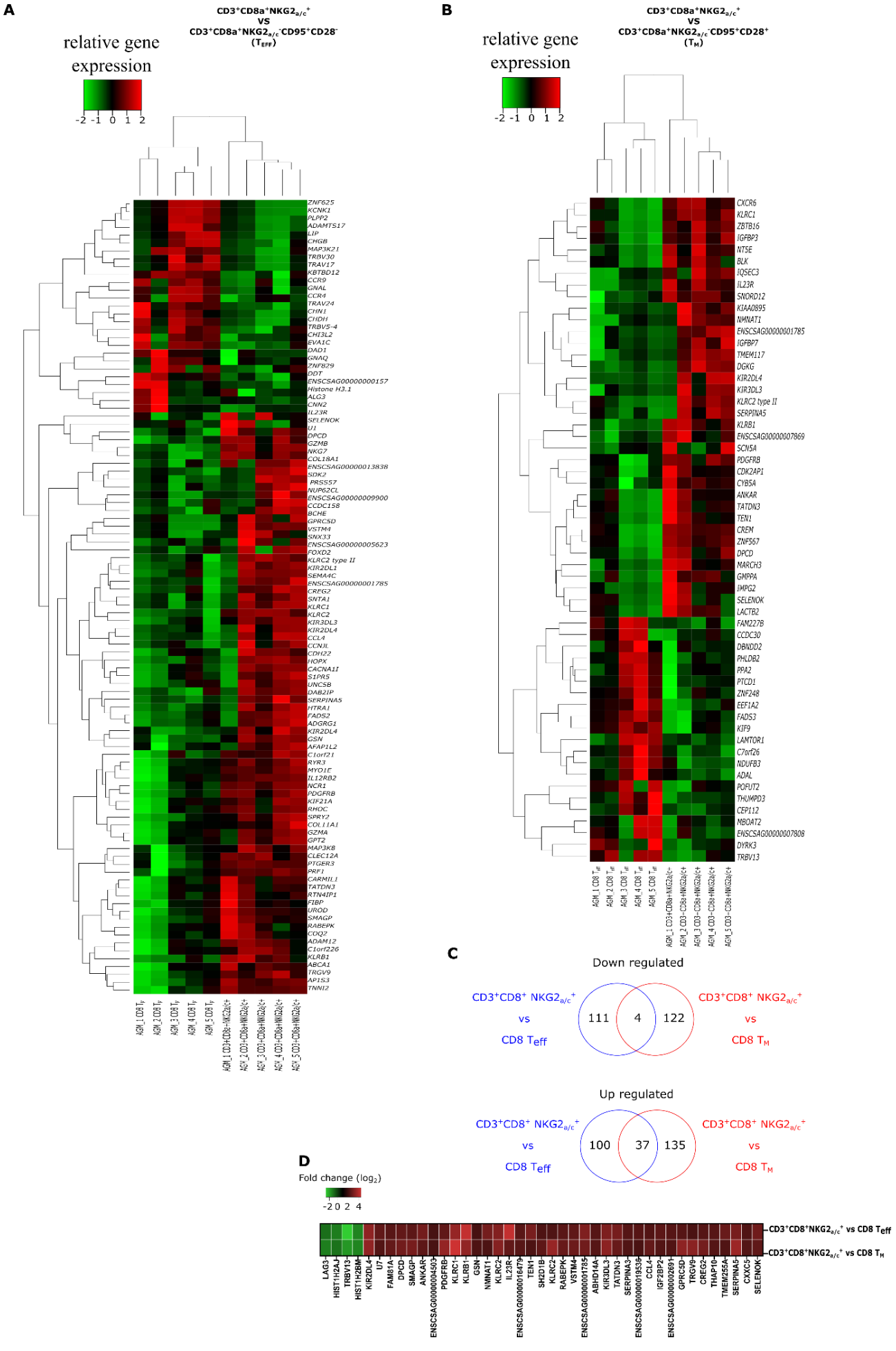
A
CD3+CD8a+NKG2a/c+
VS
CD3+CD8a+NKG2a/c-CD95+CD28-
(TEFF)
relative gene expression
-2 -1 0 1 2
B
CD3+CD8a+NKG2a/c+
VS
CD3+CD8a+NKG2a/c-CD95+CD28+
(TM)
relative gene expression
-2 -1 0 1 2
C
Down regulated
CD3+CD8+ NKG2a/c+
vs
CD8 TEff
111
4
122
CD3+CD8+ NKG2a/c+
vs
CD8 TM
Up regulated
CD3+CD8+ NKG2a/c+
vs
CD8 TEff
100
37
135
CD3+CD8+ NKG2a/c+
vs
CD8 TM
D
Fold change (log2)
-2 0 2 4
CD3+CD8+NKG2a/c+ vs CD8 TEff
CD3+CD8+NKG2a/c+ vs CD8 TM

Supplemental Figure 4. Genome-wide transcriptome analysis of NKG2$_{a/c}^{+}$CD8^{+} T cells from SIVagm-infected AGMs. Related to Figure 5. NKG2$_{a/c}^{+}$CD8^{+} T cells, conventional memory CD8^{+} T cells (CD95^{+}CD28^{+}) and conventional effector CD8^{+} T cells (CD95^{+}CD28^{-}) were sorted from blood of five chronically SIVagm-infected AGM. **(A-B)** Heat maps of unsupervised hierarchical clustering showing differentially expressed genes (**A**) between NKG2$_{a/c}^{+}$CD8^{+} T cells and conventional memory CD8^{+} T cells and (**B**) between NKG2$_{a/c}^{+}$CD8^{+} T cells and conventional effector CD8^{+} T cells. A p-value adjustment was performed to take into account multiple testing and control the false positive rate to a chosen level. The level of controlled false positive rate was set to Padj <0.05. (**C**) Venn diagrams generated by the intersection of the down- or up-regulated genes with a padj <0.05. (**D**) Unsupervised heat map showing the four down- and 37 up-regulated genes in the NKG2$_{a/c}^{+}$CD8^{+} T cells compared to both memory and effector conventional CD8^{+} T cells. The entire list of the differently transcripts are given in the supplemental tables.

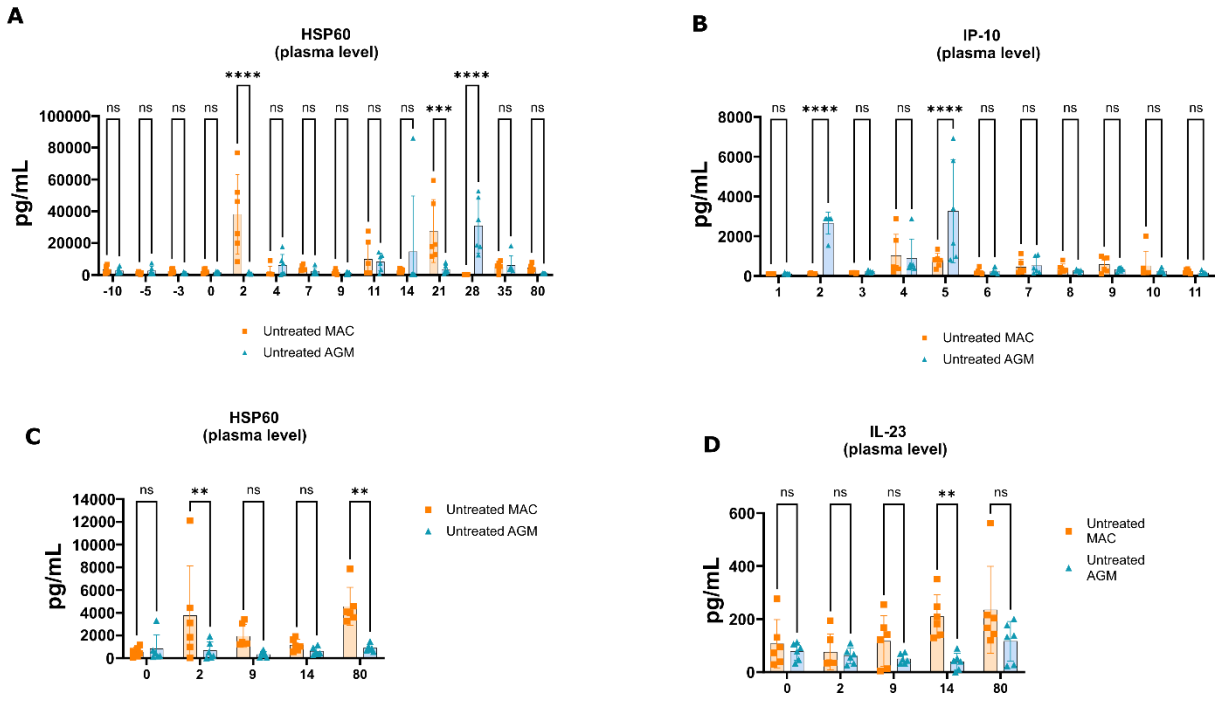

Supplemental Figure 5. Comparisons of HSP60, IP-10 and Il-23 levels measured in blood and rectal biopsies during SIV infection between AGM and MAC. Related to Figure 6. Comparison of plasma concentrations of **(A)** HSP60 and **(B**) IP-10 between AGM (blue) and MAC (orange) at the indicated time points. Comparison of **(C)** HSP60 and IL-23 **(D**) levels in cellular supernatants of unstimulated rectal biopsy cells *ex vivo* between AGM (blue) and MAC (orange) at the indicated time points. Bars represents the mean, and error bars indicate the standard deviation. Statistical significance of differences was assessed using one-way analysis of variance (ANOVA) and followed by a Tukey's multiple-comparison test. The latter is a post-hoc test based on the studentized range distribution. $*p < 0.05$, $**p < 0.005$, ***p<0.0005.

Animal #	Species	Sex	Age at inclusion (years)	SIV status	Duration after ART initiation	vRNA at necropsy (Copies/ ml plasma)	% of CD4 T cells in thawed PBMC at necropsy
AA840K	Cyn.mac	Male	7.1	ART treated	118 weeks	Indétectable	19%
AM28F	Cyn.mac	Male	7.2	ART treated	119 weeks	Indétectable	23.15%
GA342F	Cyn.mac	Male	7.1	ART treated	120 weeks	Indétectable	18.15%
SL44B	Cyn.mac	Male	7.1	ART treated	122 weeks	Indétectable	19.45%
PS6C	Cyn.mac	Male	6.5	ART treated	120 weeks	Indétectable	23.45%
CE355	Cyn.mac	Female	3.1	Viremic	n.a	4 .65E+04	15.4%
CG588	Cyn.mac	Male	2.6	Viremic	n.a	1.76E+04	10.5%
CBB001	Cyn.mac	Male	2.6	Viremic	n.a	2.08E+04	9.84%
CA797	Cyn.mac	Female	3.8	Viremic	n.a	1.30E+06	23.6%
CA552	Cyn.mac	Female	3.8	Viremic	n.a	3.69E+03	15.8%
CA275	Cyn.mac	Female	3.8	Viremic	n.a	2.19E+04	3.59%
CDI031	Cyn.mac	Female	3.3	Viremic	n.a	1.17E+06	7.67%
CDK110	Cyn.mac	Male	3.1	Viremic	n.a	9.86E+05	10.56 %
CDL093	Cyn.mac	Male	3.08	Viremic	n.a	1.93E+06	12%
CBK061	Cyn.mac	Female	5.5	Viremic	n.a	3.89E+02	8.22%
CCB028	Cyn.mac	Male	5.1	Viremic	n.a	5.06E+04	12%
CCB070	Cyn.mac	Female	5.5	Viremic	n.a	7.76E+04	6.56%
BC554D	Cyn.mac	Female	8.6	Uninfected	n.a	n.a	27.78%
BT145	Cyn.mac	Female	8.9	Uninfected	n.a	n.a	21.34%
CBL004	Cyn.mac	Male	8.6	Uninfected	n.a	n.a	31%
CC840	Cyn.mac	Male	8.4	Uninfected	n.a	n.a	27.45%
CCB116	Cyn.mac	Male	5.3	Uninfected	n.a	n.a	15.56%
RM 2153	Rh.Mac	Male	4.12	Viremic	n.a	7.E+4	1.21%
RM13909	Rh.Mac	Male	6.2	Viremic	n.a	7.91E+4	1.16%
RM8644	Rh.Mac	Male	4.7	Viremic	n.a	approx 5E+4	6.67%
RM15925	Rh.Mac	Male	5.5	Viremic	n.a	4.12^{E}+4	26.00%
RM13914	Rh.Mac	Male	6.3	Viremic	n.a	3.56^{E}+5	19.70%
RM2347	Rh.Mac	Male	6	Viremic	n.a	3.60^{E}+6	28.20%
RM14222	Rh.Mac	Male	17.7	Healthy	n.a	n.a	16.30%
RM2362	Rh.Mac	Male	5	Healthy	n.a	n.a	8.39%
RM2564	Rh.Mac	Male	7.4	Healthy	n.a	n.a	36.40%
RM14225	Rh.Mac	Male	16.9	Healthy	n.a	n.a	52.50%
RM13926	Rh.Mac	Female	6.3	Controller	n.a	< 40	23.10%
RM12671	Rh.Mac	Male	5.1	Controller	n.a	< 40	33.20%
RM2139	Rh.Mac	Male	4.6	Controller	n.a	< 40	27.50%
RM2284	Rh.Mac	Male	6.2	Controller	n.a	< 40	27.40%
RM13919	Rh.Mac	Male	5.9	Controller	n.a	< 40	12.80%
RM13923	Rh.Mac	Female	7.8	Controller	n.a	< 40	44.80%
RM2155	Rh.Mac	Male	4.4	Controller	n.a	< 40	29.40%
SV083	AGM	Male	4,97	Viremic	n.a	1 .24E+04	5.82%
SV091	AGM	Female	4,96	Viremic	n.a	1.24E+04	15.5%
SV092	AGM	Female	6,00	Viremic	n.a	1.45E+04	13%
SV101	AGM	Male	4,26	Viremic	n.a	2.37E+04	17%
SV104	AGM	Female	5,22	Viremic	n.a	2.45E+04	9.45%
SV093	AGM	Female	5,16	Viremic	n.a	5.2E+04	18.45%
SV075	AGM	Male	5,18	Uninfected	n.a	N.a	11.21%
SV1102	AGM	Male	4,36	Uninfected	n.a	N.a	9.34%
SV1201	AGM	Male	5,00	Uninfected	n.a	N.a	12.12%
SV1401	AGM	Male	3,98	Uninfected	n.a	N.a	13.24%
SV1104	AGM	Male	6,64	Viremic	n.a	1.30E+06	6.34%
SV1301	AGM	Male	5,23	Viremic	n.a	7.64E+05	8.78%
SV1303	AGM	Male	6,23	Viremic	n.a	1.94E+05	9%
SV072	AGM	Female	6,12	Viremic	n.a	3.24E+04	12.45%
SV073	AGM	Female	5,23	Viremic	n.a	5.78E+04	13.32%
SV074	AGM	Male	6.45	Viremic	n.a	2.83E+04	9.34%
SV062	AGM	Female	7.1	Viremic	n.a	1.6E+04	8%

Supplementary Table 1. Description of the animals used in the study. Related to Figure 1-6. CD4+ T cell proportions and plasma viremia levels of animals at the time point of the study, corresponding to the day of necropsy. Five CM initiated ART treatment at Week 17 following SIVmac251 infection. They belonged to the ANRS SIVART cohort.

GOID	Ontology Source	GOTerm	% Associated Genes	Term PValue	Term PValue Corrected with Bonferroni step down	Associated Genes Found
GO:0001885	GO_BiologicalProcess-EBI-UniProt-GOA_27.02.2019_00h00	endothelial cell development	4.347826	0.011987048314993875	0.05993524157496938	[CLDN1, COL18A1, HEG1]
GO:0002228	GO_BiologicalProcess-EBI-UniProt-GOA_27.02.2019_00h00	natural killer cell mediated immunity	8.974359	1.1032257318717 99E-6	6.2883866716692 54E-5	[GZMB, GZMH, KIR2DL4, KLRC2, NCR1, PVR, SH2D1B]
GO:0004896	GO_BiologicalProcess-EBI-UniProt-GOA_27.02.2019_00h00	cytokine receptor activity	4.347826	0.0012005024286238558	0.04441858985908267	[CXCR2, IL12RB2, IL15RA, IL23R, IL2RB]
GO:0007043	GO_BiologicalProcess-EBI-UniProt-GOA_27.02.2019_00h00	cell-cell junction assembly	4.4585986	1.0837452182363503E-4	0.005852224178476 2915	[ADRB2, CDH22, CLDN1, DAB2IP, HEG1, MYO1E, RHOC]
GO:0032731	GO_BiologicalProcess-EBI-UniProt-GOA_27.02.2019_00h00	positive regulation of interleukin-1 beta production	4.285714	0.012461846144211374	0.049847384576845497	[CCL3, TYROBP, XK]
GO:0034405	GO_BiologicalProcess-EBI-UniProt-GOA_27.02.2019_00h00	response to fluid shear stress	6.521739	0.0038942346933158677	0.08567316325294909	[ABCA1, ADAM12, PDGFRB]
GO:0042287	GO_MolecularFunction-EBI-UniProt-GOA_27.02.2019_00h00	MHC protein binding	5.4545455	0.006434739671822862	0.09008635540552007	[ATP5MC1, FCRL6, TRGV9]
GO:0042554	GO_BiologicalProcess-EBI-UniProt-GOA_27.02.2019_00h00	superoxide anion generation	6.122449	0.004656158665993858	0.09312317331987716	[AIFM2, BCHE, TYROBP]
GO:0060193	GO_BiologicalProcess-EBI-UniProt-GOA_27.02.2019_00h00	positive regulation of lipase activity	4.0816326	0.004700672600932 46	0.08931277941771675	[NKG7, NMUR1, PDGFRB, RHOC]
GO:0070273	GO_MolecularFunction-EBI-UniProt-GOA_27.02.2019_00h00	phosphatidylinositol-4-phosphate binding	7.142857	0.003004535964336873	0.07210886314408495	[ARHGEF40, DAB2IP, OSBPL5]
GO:0072577	GO_BiologicalProcess-EBI-UniProt-GOA_27.02.2019_00h00	endothelial cell apoptotic process	6.4102564	2.0227006172385953E-4	0.010113503086192976	[CCL4, COL18A1, DAB2IP, FASLG, SEMA4C]
GO:1904037	GO_BiologicalProcess-EBI-UniProt-GOA_27.02.2019_00h00	positive regulation of epithelial cell apoptotic process	8.0	3.863251846000 84E-4	0.018543608860804032	[CCL4, COL18A1, FASLG, GSN]
GO:2000010	GO_BiologicalProcess-EBI-UniProt-GOA_27.02.2019_00h00	positive regulation of protein localization to cell surface	14.285714	3.867819542270818E-4	0.018178751848672844	[RANGRF, SNX33, TYROBP]
KEGG:04650	KEGG_27.02.2019	Natural killer cell mediated cytotoxicity	6.8702292	3.100569372342192E-7	1.7983302359584714E-5	[FASLG, GZMB, KIR2DL4, KLRC1, KLRC2, NCR1, PRF1, SH2D1B, TYROBP]
R-HSA:419166	REACTOME_Reactions_27.02.2019	GEFs activate RhoA,B,C	7.4074073	5.193488438931458E-4	0.022851349131298413	[ARHGEF12, ARHGEF40, RHOC, TIAM2]
R-HSA:421270	REACTOME_Pathways_27.02.2019	Cell-cell junction organization	4.6875	0.009771653567550697	0.09771653567550698	[CLDN1, PVR, SDK2]
WP:623	WikiPathways_27.02.2019	Oxidative phosphorylation	4.83871	0.008958684293433222	0.10750421152119866	[ATP5MC1, GZMB, NDUFS6]

Supplemental Table 4. Table showing all pathways up-regulated between $NKG2_{a/c}^{+}CD8^{+}$ T cells and conventional memory $CD8^{+}$ T cells **Related to Figure 5.**

GOID	Ontology Source	GOTerm	% Associated Genes	Term PValue	Term PValue Corrected with Bonferroni step down	Associated Genes Found
GO:0002507	GO_BiologicalProcess-EBI-UniProt-GOA_27.02.2019_00h00	tolerance induction	9.67742	6.125632163125366E-4	0.01592664362412595	[CCR4, FOXP3, ICOS]
GO:0004896	GO_BiologicalProcess-EBI-UniProt-GOA_27.02.2019_00h00	cytokine receptor activity	6.0869565	2.9547866470393074E-6	2.2160899852794805E-4	[CCR4, CCR7, CCR9, CXCR5, IFNGR2, IL1RL1, IL9R]
KEGG:04672	KEGG_27.02.2019	Intestinal immune network for IgA production	6.122449	0.0023402692874925244	0.025742962162417768	[CCR9, CD28, ICOS]
R-HSA:3364026	REACTOME_Reactions_27.02.2019	SET1 complex trimethylates H3K4 at the MYC gene	10.810811	6.16868692768435E-9	7.464111182498064E-7	[HIST1H2AJ, HIST1H2BM, HIST1H2BN, HIST1H2BO, HIST1H3C, HIST1H3D, HIST1H4H, LEF1]
R-HSA:5083635	REACTOME_Pathways_27.02.2019	Defective B3GALTL causes Peters-plus syndrome (PpS)	8.1081085	0.001034303497677411	0.02068606995354822	[ADAMTS17, SEMA5A, SPON1]
WP:4494	WikiPathways_27.02.2019	Selective expression of chemokine receptors during T-cell polarization	13.793103	1.707156275710322E-5	0.0011096515792117093	[CCR4, CCR7, CD28, IFNGR2]

Supplemental Table 5. Table showing all pathways up- or down-regulated between $NKG2_{a/c}^{+}CD8^{+}$ T cells and conventional memory $CD8^{+}$ T cells **Related to Figure 5.**

GOID	Ontology Source	GOTerm	% Associated Genes	Term PValue	Term PValue Corrected with Bonferroni step down	Associated Genes Found
GO:0001937	GO_BiologicalProcess-EBI-UniProt-GOA_27.02.2019_00h00	negative regulation of endothelial cell proliferation	4.0	0.03125888333934946	0.03125888333934946	[CCL4, VASH1]
GO:0002230	GO_BiologicalProcess-EBI-UniProt-GOA_27.02.2019_00h00	positive regulation of defense response to virus by host	8.823529	8.701810162827896E-4	0.0417686887815739	[CISD2, IL23R, SELENOK]
GO:0002706	GO_BiologicalProcess-EBI-UniProt-GOA_27.02.2019_00h00	regulation of lymphocyte mediated immunity	4.4198895	7.55541956823745E-6	4.684360132307219E-4	[HAVCR2, IL18RAP, IL23R, KIR2DL4, NECTIN2, PARP3, PGAP2, SH2D1B]
GO:0007000	GO_BiologicalProcess-EBI-UniProt-GOA_27.02.2019_00h00	nucleolus organization	25.0	8.307247081446358E-4	0.040705510699087157	[EMG1, RRN3]
GO:0033198	GO_BiologicalProcess-EBI-UniProt-GOA_27.02.2019_00h00	response to ATP	4.0816326	0.0301154484631127	0.0602308969262254	[P2RY11, SELL]
GO:0034706	GO_CellularComponent-EBI-UniProt-GOA_27.02.2019_00h00	sodium channel complex	6.6666665	0.011922019122552217	0.22651836332849212	[GRIK4, SCN5A]
GO:0051974	GO_BiologicalProcess-EBI-UniProt-GOA_27.02.2019_00h00	negative regulation of telomerase activity	14.285714	2.0379652147891909E-4	0.01080121563838271	[CCL4, PARP3, TEN1]
GO:0070475	GO_BiologicalProcess-EBI-UniProt-GOA_27.02.2019_00h00	rRNA base methylation	18.181818	0.0016141598572718167	0.07263719357723175	[EMG1, METTL15]
GO:1990166	GO_BiologicalProcess-EBI-UniProt-GOA_27.02.2019_00h00	protein localization to site of double-strand break	50.0	1.8061201312994564E-4	0.009933660722147011	[PARP3, SLF1]
R-HSA:198933	REACTOME_Pathways_27.02.2019	Immunoregulatory interactions between a Lymphoid and a non-Lymphoid cell	5.263158	9.223647161178101E-6	5.626424768318642E-4	[KIR2DL4, KLRB1, KLRC1, NECTIN2, SELL, SH2D1B, SIGLEC6]
R-HSA:380108	REACTOME_Pathways_27.02.2019	Chemokine receptors bind chemokines	4.1666665	0.028989214286469226	0.08696764285940768	[CCR6, CXCR6]
R-HSA:5633008	REACTOME_Pathways_27.02.2019	TP53 Regulates Transcription of Cell Death Genes	4.5454545	0.024660773437397414	0.14796464062438447	[IGFBP3, PERP]
R-HSA:8865265	REACTOME_Reactions_27.02.2019	TFAP2C homodimer binds MYC and KDM5B	66.666664	9.063425410090201E-5	0.005075518229650512	[KDM5B, MYC]
WP:3644	WikiPathways_27.02.2019	NAD+ metabolism	12.5	0.003458754124243925	0.12797390259702524	[NMNAT1, NT5E]

Supplemental Table 6. Table showing all pathways up-regulated between $NKG2_{a/c}^{+}CD8^{+}$ T cells and conventional memory $CD8^{+}$ T cells **Related to Figure 5**.

Antibody	Clone	Suppliers	Control
CD3	SP34-2	BD biosciences	Isotype + FMO
CD45	D058-1283	BD biosciences	Isotype + FMO
CD20	2H7	Biolegend	Isotype + FMO
NKG2A/C	Z199	Beckman Coulter, Inc.	Isotype + FMO
CD16	3G8	Beckman Coulter, Inc.	Isotype + FMO
CXCR5	710D82.1	NHP reagent	Isotype + FMO
CD8	BW135/80	Miltenyi	Isotype + FMO
CD4	L200	BD biosciences	Isotype + FMO
CXCR3	1C6/CXCR3	BD biosciences	Isotype + FMO
NKp80	4A4.D10	Miltenyi	Isotype + FMO
NKP30	AF29-4D12	Miltenyi	Isotype + FMO
CD279 (PD-1)	EH12.2H7	BD biosciences	Isotype + FMO
CD107a	H4A3	BD biosciences	Isotype + FMO
CD28	CD28.2	BD biosciences	Isotype + FMO
CD95	DX2	BD biosciences	Isotype + FMO
CD69	FN50	BD biosciences	Isotype + FMO
HLA-DR	TU36	BD biosciences	Isotype + FMO
PRF1	PF-344	mabtech	Isotype + FMO
CXCR3	1C6/CXCR3	BD biosciences	Isotype + FMO
CCR7	3d12	eBioscience	Isotype + FMO
CD62L	150503	R&D	Isotype + FMO
CX3CR1	2a9-1	biolegends	Isotype + FMO
CXCR5	MU5UBEE	eBioscience	Isotype + FMO
NKG2d	ON72	Beckman Coulter, Inc	Isotype + FMO
NKP46	BAB281	Beckman Coulter, Inc	Isotype + FMO
NKP44	2.29	Miltenyi	Isotype + FMO
Ki-67	MIB-1	Dako	Isotype + FMO
CD107a	H4A3	BD biosciences	Isotype + FMO
TNF-a	MAb11	BD biosciences	Isotype + FMO
IFN-g	45-15	Miltenyi	Isotype + FMO

Supplemental Table 7. Related to Figure 1-6. Antibodies used for flow cytometry.

Transparent Methods

Monkeys and SIV infections

Seventeen African green monkeys (Caribbean *Chlorocebus sabaeus,* AGM), twenty-two cynomolgus macaques (*Macaca fascicularis,* CM) and 17 rhesus macaques (*M. mulatta*, RM) were included in the study. Twelve AGM were infected with SIVagm.sab92018, 17 CM with the SIVmac251 and 13 RM with the SIVmac239 as previously described (Diop et al., 2000; Huot et al., 2017; Jacquelin et al., 2009). The ART-treated CM are part of the SIVART cohort from the ANRS. Animals received ART regimen once daily at 1 ml kg-1 body weight via the subcutaneous route with TDF administered at 5.1 mg/kg, FTC at 40 mg/kg and DTG at 2.5 mg/kg. Treatment was initiated 17 weeks p.i. All ART-treated animals were virologically suppressed at the time of this study. Viral load in AGM, CM and RM was quantified as previously described (Huot et al., 2017; Jacquelin et al., 2014). The viremia and CD4+ T cell levels of the animals are given in Supplementary Figure 2 and Supplemental Table 1.

The AGM and CM were housed at the IDMIT Center (Fontenay-aux-Roses, France) and the RM at the German Primate Center (DPZ). All experimental procedures were conducted in strict accordance with the international European guidelines 2010/63/UE on the protection of animals used for experimentation and other scientific purposes, with the German and French law (French decree 2013-118) and the recommendations of the Weatherall report. The IDMIT center complies with the Standards for Human Care and Use of the Office for Laboratory Animal Welfare (OLAW, USA) under OLAW Assurance number A5826-86. The DPZ has the permission to breed and house NHPs under license number 392001/7 granted by the local veterinary office and conforming with §11 of the German Animal Welfare act. Monitoring of the monkeys was under the supervision of the veterinarians in charge of the animal facilities. The animals used here were shared with other studies (Huot et al., 2017)·(Huot et al., 2020). Animal experimental protocols were approved by the Ethical Committee of Animal Experimentation (CETEA-DSV, IDF, France) (Notification 12-098, 16_010, APAFIS#11236-2017091214402801 v1, and number A15-035 by the ethics committee "*Comité d'Ethique en Expérimentation Animale du CEA")*, registered and authorized under Number 2453-2015102713323361v2 by the French Ministry of Education and ResearchThe study at DPZ was approved by the Lower Saxony State Office for Consumer Protection and Food Safety and performed with the project licences 33.19-42502-04-12/0820 and 33.19-42502-04-17/2500. The DPZ has the permission to breed and house nonhuman primates under license number 392001/7 granted by the local veterinary office and conforming with § 11 of the German Animal Welfare act.

The animals were healthy and seronegative for SIV, type D retrovirus, and simian T-cell lymphotropic virus type 1 at the time of infection and were housed in single cages within level 3 biosafety facilities after infection. At the inclusion in the study the average weight of the monkeys was between 3 and 7 kg. All monkeys were young adults at inclusion (supplemental

table 1). Both males and females were used. Because H6 haplotypes are notably associated with viral control in cynomolgus macaques, macaques with H6 haplotype were excluded from this study.

Monkeys were sedated with Ketamine Chlorhydrate (Rhone-Mérieux, Lyons, France) before handling. The sample size varied between 3 and 9 monkeys per group (n = 6 in most experiments). Sample collection was performed in random order, according to the tripartite harmonized International Council for Harmonization of Technical Requirements for Pharmaceuticals for Human Use (ICH) Guideline on Methodology (previously coded Q2B). The investigators were not blinded while the animal handlers were blinded to group allocation.

Tissue collection and processing for flow analysis

Whole blood was collected in EDTA tubes. Mononuclear cells were isolated by Ficoll density-gradient centrifugation. Lymph node and rectal biopsies were collected longitudinally before and during infection. The other tissues were collected at autopsy and cleaned of adhering connective and fat tissues. Fractions of the ileum, jejunum and colon were removed immediately after sacrifice, trimmed free of adjacent tissue and cleaned of stool. Adhering connective and fat tissues were carefully removed and approximately 7 cm intestinal pieces were placed in PBS supplemented with 20 % of SVF, 1.0%Glutamine, 0.8% antibiotics/antimycotics (all Sigma-Aldrich, St Louis, MO), 1 mM dithiothreitol (Roth, Karlsruhe, Germany) and 1.5 mM EDTA (Roth) and then cut in little pieces with scissors. Cells were dissociated using the gentleMACS™ Dissociator technology (Miltenyi Biotec, Germany). The suspensions were centrifuged (7 min, 300g, RT) and cell pellets were re-suspended in DMEM containing fetal calf serum, L-glutamine and antibiotics. For each tissue cell suspension was filtrated subsequently through 100- and 40-µm cell strainers, and cells were washed with cold PBS. Cells were either immediately stained for flow cytometry or cryopreserved in 90% FBS, 10% DMSO and stored in liquid nitrogen vapor.

Polychromatic flow cytometry

Cells were stained as previously described (Huot et al., 2017). Briefly, FcR blocking reagent (Miltenyi) was used to block unspecific antibody binding. Antibodies used are shown in Supplemental Table 7. The anti-CD8 monoclonal antibody corresponded to BW135/80 (Miltenyi), staining CD8a. Flow cytometry acquisitions were performed on an LSR II (BD Biosciences). Intra-cellular staining was performed using BD Cytofix/Cytoperm™. Intracellular cytokines were measured *ex vivo* without prior *in vitro* stimulation. The data were further analyzed using FlowJo 10.4.2 software (FlowJo, LLC, Ashland, OR, USA). *t*-SNE (*t*-distributed stochastic neighbor embedding) was carried out using the *t*-SNE feature in FlowJo using 2000 iterations and a perplexity of 50.

Cell sorting

Cells were thawed in 20% fetal bovine serum-containing media supplemented with Benzonase nuclease, washed and stained with Aqua Live/Dead stain (Molecular Probes). Cell counts and viabilities were determined (Life Technologies). After a washing step, cells were blocked using normal mouse IgG (Caltag). Cells were surface-stained for CD3 (SP34-2, dilution 1/10, BD), CD8 (BW135/80, dilution 1/20, Miltenyi), CD95 (DX2, dilution 1/20, BD), NKG2a/c (Z199, dilution 1/20, Beckman Coulter, Inc.), CD20 (2H7, dilution 1/20, Biolegend), CD14 (M5E2, dilution 1/25, BD) and CD28 (CD28.2, dilution 1/20, BD). Post-surface staining, cells were washed, filtered and $CD45^{+}CD14^{-}CD20^{-}CD3^{+}$ effector ($NKG2_{a/c}^{-}CD28^{-}CD95^{+}$), memory ($NKG2_{a/c}^{-}CD28^{+}CD95^{+}$) and $NKG2_{a/c}^{+}$ $CD8^{+}$ T cells sorted on a FACS ARIA II (BD Biosciences). Cells were directly collected in a lysis buffer containing TCEP. All samples were re-examined by flow cytometry following sorting, to ensure purity above 99%.

Hsp60, IL-23 and IP-10 quantification

Hsp60, IL-23 and IP-10 were quantified in plasma and supernatants of tissue biopsies. After biopsy, the tissues were transported to the laboratory and kept during the transport for 2-3 hours at 4°C in RPMI medium. The tissues were then cut into pieces, grinded with a gentleMACS Dissociator (Miltenyi Biotec, 130-093-235) in 500µl of RPMI per biopsy of similar size. The tissue cell suspension was centrifugated at 1500g for 5 min to pellet the cells. The cells were used fresh or were frozen in FBS with 10% of DMSO and stored in liquid nitrogen until further use. The supernatants were filtered at 70µm (Clearline, 141379C), centrifugated (1000g for 20 min) to clean from remaining cell debris and then stored at -80°C. The proteins were quantified using the Mouse HSP60 ELISA Kit (AbCAM), Monkey IL-23 ELISA kit, U-CyTech biosciences and the Human CXCL10/IP-10 Quantikine ELISA Kit R&D systems, according to the provider's instructions.

RNA-seq profiling

RNA was isolated from the sorted cells using the RNeasy® Plus Micro Kit (74034, Qiagen). RNA integrity was verified with the Agilent Bioanalyzer. RNA molecules were treated for library preparation using the Truseq Stranded mRNA sample preparation kit (Illumina, San Diego, California) according to manufacturer's instructions. An initial poly(A) RNA isolation step (included in the Illumina protocol) was performed on 10 ng of total RNA to keep only the polyadenylated RNA fraction and remove the ribosomal RNA. A step of fragmentation was applied on the enriched fraction by divalent ions at high temperature. The fragmented RNA samples were randomly primed for reverse transcription followed by second-strand synthesis to create double-stranded cDNA fragments. No end repair step was necessary. An adenine was added to the 3'-end and specific Illumina adapters were ligated. Ligation products were submitted to PCR amplification. The obtained oriented libraries were controlled by Bioanalyzer DNA1000 Chips (Agilent, # 5067-1504) and quantified by spectrofluorimetry (Quant-iT™

High-Sensitivity DNA Assay Kit, #Q33120, Invitrogen). Sequencing was performed on the Illumina Hiseq2500 platform to generate single-end 100 bp reads bearing strand specificity.

RNA-seq data analyses

Reads were cleaned of adapter sequences and low-quality sequences using cutadapt version 1. 1162.Bowtie version 1.2.2, with default parameters, was used for alignment of reads on the reference genomes (*Chlorocebus sabaeus* from Ensembl release 90). Genes were counted using HTseq-count version 0.11.1. Count data were analyzed using R version 3.4.361 and the Bioconductor package DESeq2 version 1.18.162. The normalization and dispersion estimation were performed with DESeq2 using the default parameters and statistical tests for differential expression were performed applying the independent filtering algorithm. For each comparison, p-values were adjusted for multiple testing according to the Benjamini and Hochberg procedure and genes with an adjusted p-value lower than 0.05 were considered as differentially expressed. Heatmaps representations were generated based on the rescaled gene expression levels. Hierarchical clustering, shown as dendrograms on the top and on the left of the heatmaps, were generated based on the Euclidian distance and using the complete linkage method.

Functional Enrichment analysis

Analyses and visualization of GO terms associated with differentially expressed genes were performed using ClueGO**.** Both groups of genes (up- and downregulated, p value < 0.05 and fold change >2) were used as dual input for GO and pathway annotation networks of the expressed genes and proteins pathway enrichment analysis (Bindea et al., 2009). Each list was used to query the Kyoto Encyclopedia of Genes and Genomes (KEGG), GO-biological function database, REACTOME and Wiki pathways. ClueGo parameters were set as follows: Go Term Fusion selected; only display pathways with p values $\leqslant$ 0.05; GO tree interval, all levels; GO term minimum genes, threshold of 4% of genes per pathway; and a kappa score of 0.42. GO terms are presented as nodes and clustered together based on the similarity of genes present in each term or pathway. The most significant term was chosen as a representative of the group (Benjamini-Hochberg correction).

Statistical analyses

The GraphPad Prism 7 (GraphPad Software, San Diego, CA) was used to analyze data and to perform statistical analyses. Statistical significance of differences was assessed using non-parametric Mann-Whitney *U* tests (Figure 1, Figure 4C, G, H), or Wilcoxon matched-pairs signed rank test, for paired samples (Figure 4 A,D,E,F). All group comparisons were carried out by means of a one-way analysis of variance (ANOVA) and followed by a Tukey's multiple-comparison test. The latter is a post-hoc test

based on the studentized range distribution (Figure2, Figure3, Figure 4 B, L, K, M and Figure 6). Values of $p < 0.05$ were considered significant. Correlation analyses were performed according to the Spearman or Pearson coefficient of correlation.